Effect of rigid connection to an asymmetric building on the random seismic response

Hamed Ahmadi Taleshian*, Alireza Mirzagoltabar Roshan and Javad Vaseghi Amiri

Department of Civil Engineering, Noshirvani University of Technology, Babol, Iran

Abstract. Connection of adjacent buildings with stiff links is an efficient approach for seismic pounding mitigation. However, use of highly rigid links might alter the torsional response in asymmetric plans and although this was mentioned in the literature, no quantitative study has been done before to investigate the condition numerically. In this paper, the effect of rigid coupling on the elastic lateral-torsional response of two adjacent one-story column-type buildings has been studied by comparison to uncoupled structures. Three cases are considered, including two similar asymmetric structures, two adjacent asymmetric structures with different dynamic properties and a symmetric system adjacent to an adjacent asymmetric one. After an acceptable validation against the actual earthquake, the traditional random vibration method has been utilized for dynamic analysis under Ideal white noise input. Results demonstrate that rigid coupling may increase or decrease the rotational response, depending on eccentricities, torsional-to-lateral stiffness ratios and relative uncoupled lateral stiffness of adjacent buildings. Results are also discussed for the case of using identical cross section for all columns supporting each plan. In contrast to symmetric systems, base shear increase in the stiffer building may be avoided when the buildings lateral stiffness ratio is less than 2. However, the eccentricity increases the rotation of the plans for high rotational stiffness of the buildings.

Keywords: rigid link; random vibration; torsion; dynamic properties; response ratio

1. Introduction

Whenever the static distance between adjacent buildings is insufficient for impact prevention, pounding mitigation techniques are suitable remedies for reducing the detrimental effects of pounding (Abdel Raheem *et al.* 2019, Jin and Yang 2018, Soltysik *et al.* 2017). A comprehensive study on seismic pounding mitigation procedures has been carried out by Miari *et al.* (2019) and Jankowski and Mahmoud (2015). In contrast to bridges, where effects such as the difference in propagation of seismic waves (Chouw and Hao 2005) or even the fluid-structure interaction at deep-water piers (Deng *et al.*(2018) might be attributed to pounding, different dynamic properties are the main factor in buildings. In this regard, connecting the adjacent buildings with links having limited stiffness but certain amount of energy dissipation would be a promising solution. Such links are generally classified into three groups according to the literature, namely Viscous, Viscoelastic and Magno-Rheological dampers. A state-of-the-art on damper for seismic connection has been presented by Passoni *et al.* (2014). Among the first group studies, Patel and Jangid (2010) studied the dynamically similar adjacent structures connected by viscous dampers, while Luco and De

---

*Corresponding author, Ph.D. Student, E-mail: hamed_ahmadi0111@yahoo.com

Barros (1998) and Kandemir-mazanoglu and Mazanoglu (2017) persued the optimization of such damper connections. The seismic performance of the buildings connected by fluid dampers has been studied by Xu *et al.* (1999) and Abd-elsalam *et al.* (2012). Among the studies attributed to viscoelastic connection, Zhu and Iemura (2000) investigated the connection modeled with a spring and a dashpot that act in parallel. An optimization study for a series interrelation of connection stiffness and damping has been studied by Zhu and Xu (2005). Mirzagoltabar Roshan *et al.* (2017) compared two cases of viscous and viscoelastic connections for seismic pounding mitigation, in which both connections were found to be effective tools. Investigation of the viscoelastic links under random seismic input has been carried out by Ahmadi Taleshian *et al.* (2019). The efficiency of viscous and viscoelastic dampers is also verified by Izharulhaque and Shinde (2016). Comparison of different pounding mitigation techniques has also been studied by Jankowski and Mahmoud (2016), where the linking of adjacent buildings was found to be a satisfactory solution. Kim *et al.* (2006) studied the seismic behavior of adjacent buildings connected by viscoelastic dampers. Abdel-Mooty and Ahmed (2017) considered viscoelastic dampers for localized connection between separated parts of a building. Bharti *et al.* (2010) and Abdeddaim *et al.* (2016, 2017) studied the Magno-Rheological dampers as a more recent seismic pounding mitigation technique. Perez *et al.* (2017) has proved the efficiency of connection with energy dissipation property through experimental study and Pratesi *et al.* (2014) practically used dampers for pounding mitigation of an ancient tower against its adjacent structure. In spite of the advantages and efficiencies of less-stiff energy-dissipater connections, there are some cases that less costly rigid connection can be used, if the dynamic characteristics of the coupled system are fully understood. This case is particularly important in the connection of asymmetric buildings, where using links with high rigidities might alter the torsional effects on the adjacent structures. This depends on dynamic properties such as eccentricities, as well as relative lateral and torsional stiffness (frequencies) of buildings and though past publications, such as Westermo (1989) and Xu *et al.* (1999), have notified the possibility of increase in torsional response due to rigid connection and even the importance of transferred torsion between different parts of the integrated system was emphasized since the 1970s (Ban 1973) and also considering the more critical condition induced by torsion in moment resisting frames (Abdel Raheem *et al.* (2018)), few detailed numerical works have been done so far to investigate the condition more profoundly. Only recently, Hu *et al.* (2018) investigated the effect of links on the acceleration response of the connected 3D buildings under wind excitation, where they found that the translational acceleration response decreases by increasing the stiffness of links, with torsional acceleration may exceed that of unlinked case.

The uncertain nature of earthquakes has made random vibration analysis increasingly popular, where it is common to account the uncertainty only for input excitation by considering the structural properties to be deterministic. One of the simplest cases of stationary stochastic loading is to model the excitation as ideal white noise in which same probabilistic weight would be assigned for all possible frequencies to be as the input. Although such an assumption is not physically realizable and does essentially differ from characters of probable excitations from both amplitude and frequency content points of view, it has been widely used in the dynamic analysis. It has been made clear under white noise analysis that near 80% of the root of the mean-squared displacement in a lightly-damped SDOF system would be obtained by a small band around the natural frequency (Nigam 1983) and frequencies more than twice the natural one would have negligible effects on probable response (Crandall and Mark 1963). Even when the input power spectral density (PSD) has peak values much larger than its value at the natural frequency, which of course is inconsistent with the findings of the critical excitation method (Takewaki 2013), acceptable results were obtained
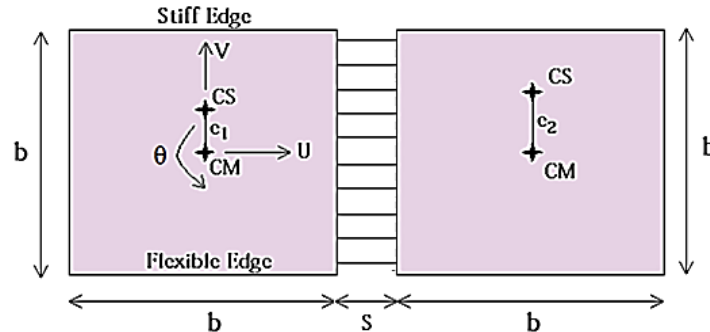
Fig. 1 Plans of the linked buildings

by equivalent white noise for structures damped less than 5% of critical (Lutes and Sarkani 2004). These significations, together with past attempts for matching earthquakes with constant PSD values, as investigated by Bycroft (1960), verify the adequacy of white noise analysis for systems with light damping.

In this paper, two one-story buildings with transnationally and rotationally rigid in-between connection have been analyzed under white noise input. Although multi-story models are more accurate, past studies legitimated the use of simpler one-story models by admitting that it can realize the behavior, at least qualitatively, in lights of careful selection of dynamic properties (Anagnostopolous *et al.* 2010). The rigid connection mentioned herein is practically achieved by means of axially-stiff members with high rigid end connections, as discussed intensively in the literature, such as Imamovic *et al.* (2019), Ibrahimbegovic and Ademovic (2019), Ibrahimbrgovic *et al.* (2014) and Ibrahimbegovic and Mamouri (2000). After performing Eigen-analysis for determining natural frequencies and mode shapes of the integrated system, the stationary responses of interest such as rotation and displacement at important positions would be first calculated and then compared with unlinked results by means of computing linked-to-unlinked response ratios.

2. Modeling and formulation

The plans of two adjacent one-story lumped- mass asymmetric buildings of equal heights linked by rigid massless elements are depicted in Fig. 1. Each rigid diaphragm is supported by a collection of square-section elastic RC columns, leading to equal stiffness of buildings in both horizontal directions. The motivation for choosing plans with equal dimensions is to assure the suitable behavior by avoiding the localization of interactions that would be relevant for small or large aspect ratios of adjacent plans. The buildings are assumed to have uniform mass distribution, i.e. center of mass coincides with the geometric center. The fictitious line connecting centers of plans is also assumed to be aligned with link elements. It should be noted that macro-modeling of real RC structures would alter the overall stiffness of the system, compared to that in micro-scale Finite element programs (Abdel Raheem *et al.* 2018). Such effects are not considered in this paper.

The presence of both axially and rotationally rigid connection reduces the whole system to a 3-DOFs one, with two translations and one rotation about the axes perpendicular to the plan. For the sake of simplicity, unidirectional excitation parallel to link elements was applied and the buildings were defined to have stiffness eccentricities only in the direction perpendicular to the excitation, as

shown in Fig. 1. These assumptions may reduce the model to 2-DOFs one with the following equation of motion (Eq. (1)), in which identical ground acceleration is considered for both buildings and the soil-structure interaction was ignored, while the horizontal shear transfer was allowed between plans: (See Appendix for more details)

$$
\begin{bmatrix} m_1 + m_2 & 0 \\ 0 & I_1 + I_2 + m_2.L^2 \end{bmatrix} \begin{bmatrix} \ddot{u} \\ \ddot{\theta} \end{bmatrix} + [C] \begin{bmatrix} \dot{u} \\ \dot{\theta} \end{bmatrix}
$$
$$
+ \begin{bmatrix} k_{x1} + k_{x2} & k_{x1}.e_1 + k_{x2}.e_2 \\ k_{x1}.e_1 + k_{x2}.e_2 & k_{\theta 1} + k_{\theta 2} + k_{y1}.k_{y2}.L^2/(k_{y1} + k_{y2}) \end{bmatrix} \begin{bmatrix} u \\ \theta \end{bmatrix} = -\begin{bmatrix} m_1 + m_2 \\ 0 \end{bmatrix}.\ddot{X}_g
$$
(1)

Where U and θ are, respectively, translational and rotational DOFs of the system measured at the center of mass of the left building, L denotes the distance between centers of mass in adjacent plans: $L = b + S$ (Fig. 1), $\ddot{X}_g$ is the ground acceleration and m_j, I_j, K_{xi}, K_{yj} and $K_{\theta j}$ ($j=1,2$) are mass, moment of inertia, translational stiffnesses (parallel to excitation and perpendicular to that) and torsional stiffness about the center of mass of building j, respectively. e_j stands for the stiffness eccentricity of building j, which is more convenient to be expressed as a fraction of the co-directional plan dimension, i.e., $e_j'=e_j/b$. The damping matrix $[C]$ is not explicitly defined in Eq. (1), as the classical damping condition is acceptable here in a system with no supplemental energy dissipation. In this study, 5% of the critical damping is applied in different modes of vibration (Chopra 1995). By assuming $m_1=m_2=m$ in order to focus only on stiffness changes, neglecting the gap size with respect to plan dimension, i.e., $s/b\approx0$ (This is typical in pounding-concerned cases) and recalling the definition of the moment of inertia for rectangular plans, Eq. (1) can be rewritten as

$$
\begin{bmatrix} 2m & 0 \\ 0 & \frac{4}{3}mb^2 \end{bmatrix}.\begin{bmatrix} \ddot{u} \\ \ddot{\theta} \end{bmatrix} + [C]\begin{bmatrix} \dot{u} \\ \dot{\theta} \end{bmatrix} + \begin{bmatrix} k_{x1} + k_{x2} & k_{x1}.e_1 + k_{x2}.e_2 \\ k_{x1}.e_1 + k_{x2}.e_2 & k_{\theta 1} + k_{\theta 2} + b^2/(1/k_{x1} + 1/k_{x2}) \end{bmatrix}\begin{bmatrix} u \\ \theta \end{bmatrix} = -\begin{bmatrix} 2m\ddot{X}_g \\ 0 \end{bmatrix}
$$
(2)

Note that the assumption of $K_{xi}=K_{yi}$ mentioned before, together with other mentioned assumptions, results in $L=b$ used in simplifying Eq. (1) and subsequent extraction of Eq. (2). According to the classical Random Vibration theory, the stationary expected value of the squared response of a single mode i of vibration under mean-zero white noise excitation can be stated as follows

$$
E[U_i^2] = \frac{L_i^2}{M_i^2}.\frac{\pi S_0}{2\xi_i\omega_i^3}
$$
(3)

Where S_0 is the constant PSD of the ground acceleration and L_i, M_i, ω_i and ξ_i are modal excitation factor, modal mass, natural frequency and damping ratio of the mode, respectively. Also, the term denoting interaction of different modes i and j shall be calculated as

$$
E[U_i U_j] = \frac{L_i.L_j}{M_i.M_j}.\frac{4\pi(\xi_i\omega_i + \xi_j\omega_j).S_0}{[(\omega_i^2 - \omega_j^2)^2 + 4\omega_i\omega_j(\xi_i\omega_i + \xi_j\omega_j)(\xi_i\omega_j + \xi_j\omega_i)]}
$$
(4)

When damping is small and the natural frequencies are not closely spaced, values from eq.4 are much smaller than the mean values from Eq. (3). Once the expected values were obtained, modal transformation can be used for attaining the results of interest as

$$E[U^2] = E[U_1^2] + E[U_2^2] + 2.E[U_1.U_2] \tag{5}$$

$$E[\theta^2] = \Phi_{12}^2.E[U_1^2] + \Phi_{22}^2.E[U_2^2] + 2.\Phi_{12}.\Phi_{22}.E[U_1.U_2] \tag{6}$$

In which Φ_{12} and Φ_{22} are the associated elements of the mode shape matrix. To facilitate comparison with the case of no torsional coupling, displacement at the center of rigidity is required, which would be as follows

$$E[\Delta_{CS}^2] = E[(U - e_1.\theta)^2] = E[U^2] + e_1^2.E[\theta^2] - 2e_1.E[U.\theta] \tag{7}$$

Where

$$E[U.\theta] = \Phi_{12}.E[U_1^2] + \Phi_{22}.E[U_2^2] + (\Phi_{12} + \Phi_{22}).E[U_1.U_2] \tag{8}$$

The obtained results should be compared to those of the separated left building in Fig. 1, with the following equation of motion

$$\begin{bmatrix} m & 0 \\ 0 & \frac{1}{6}mb^2 \end{bmatrix}\begin{bmatrix} \ddot{u}' \\ \ddot{\theta}' \end{bmatrix} + [C'].\begin{bmatrix} \dot{u}' \\ \dot{\theta}' \end{bmatrix} + \begin{bmatrix} k_{x1} & k_{x1}.e_1 \\ k_{x1}.e_1 & k_{\theta 1} \end{bmatrix}\begin{bmatrix} u' \\ \theta' \end{bmatrix} = -\begin{bmatrix} m \\ 0 \end{bmatrix}.\ddot{X}_g \tag{9}$$

Prime (') denotes the corresponding values for a single unlinked building. After performing Eigen-analysis, the expected values of interest may be calculated as follows

$$E[\theta'^2] = \Phi'_{12}^2.E[U'_1^2] + \Phi'_{22}^2.E[U'_2^2] + 2.\Phi'_{12}.\Phi'_{22}.E[U'_1.U'_2] \tag{10}$$

$$E[\Delta'_{CS}^2] = E[U'^2] + e_1^2.E[\theta'^2] - 2e_1.E[U'.\theta'] \tag{11}$$

3. Definition of the parametric study

This study is planned to be carried out in three different parts, with the eccentricity and relative lateral and torsional stiffness of adjacent buildings as the main varying parameters. In the first part of the study noted as part A, the adjacent buildings are assumed to have identical structural properties, i.e., same lateral and torsional stiffness and also similar eccentricities. This part is less significant from pounding point of view due to in-phase motions of the buildings and no load transfer would thus be anticipated if symmetric plans were to be used. However, eccentricities and subsequent torsion may pose the applicability for the strengthening of adjacent structures under question. The second part of the study (part B) deals with two asymmetric-plan buildings with various dynamic properties. Finally and at part C, One of the plans would be considered symmetric in order to cover a new aspect of torsional coupling that is only induced by a rigid connection to the adjacent eccentric structure and will be omitted by removing the connection. It should be noted that eccentric pounding may induce rotation for both symmetric (Abdel Raheem *et al.* 2019, Leibovich

et al. 1996) and asymmetric (Wang and Chau 2008) plans, but this type of torsional coupling would not be addressed in this paper.

In the next part of the paper,   results would be presented in either tabular or graphical formats for different values of eccentricities, relative lateral and torsional stiffness and dimensionless torsional-to-lateral stiffness ratios, $\alpha=K_{\theta 1}/(b^2.K_{x1})$, of the buildings. Note that the definition of α varies in different research studies due to current literature (Chakroborty and Roy 2016, Chiba and Magata 2019, Anagnostopoulos *et al.* 2015), but the current definition has the merit of determining its bounds more directly. The upper bound would be 0.5, as if a diaphragm is only supported by columns at four corners. On the other hand, the practical value of 0.2 is a suitable choice for the lower bound, although a minimum of zero is pathologically possible by only using one column at the plan center. These two bounds, as representatives of high ($\alpha=0.5$) and low ($\alpha=0.2$) torsional rigidity, together with a moderate value of $\alpha=0.35$, would be used in the paper.

4. Results and discussion

4.1 Part A

Results of the two adjacent similar SDOF system for $\alpha=0.5$ is tabulated in Table 1, where the first column is the identical eccentricity ratios, $e'=e/b$, of adjacent buildings, the next two columns are the natural frequencies of the first and second modes of vibration that are expressed as dimensionless factors of the left building's uncoupled natural frequency, $\omega_0 = (K_{x1}/m_1)^{0.5}$. Columns 4 and 5 are the same as columns 2 and 3, but for a single unlinked building. The stationary expected values of squared rotation and displacement at the center of rigidity have been presented, respectively in columns 6 and 7 for connected buildings and in columns 8 and 9 for a separated building. These expected values of rotation and displacement have been respectively normalized by $\pi S_0/(\xi.m^2.\omega_0^3.b^2)$ and $\pi S_0/(\xi.m^2.\omega_0^3)$, with $\xi=0.05$. Finally, the ratios of the square roots of the responses in the two different cases are given in the last two columns of the Table. These dimensionless quantities may be regarded as the probabilistic representatives of the linked-to-unlinked response ratios.

At this moment, it may be of practical interest to compare the results with actual broadband

Table 1 Results of analysis for $\alpha=0.5$ with respect to the identical eccentricities of buildings ($e'=e_1=e_2$)

| e'	ω_1 $(\times\omega_0)$	ω_2 $(\times\omega_0)$	ω'_1 $(\times\omega_0)$	ω'_2 $(\times\omega_0)$	$E(\theta^2)$	$E(\Delta_{CS}^2)$	$E(\theta'^2)$	$E(\Delta'_{CS}^2)$	$\sqrt{\dfrac{E[\theta^2]}{E[\theta'^2]}}$	$\sqrt{\dfrac{E[\Delta_{CS}^2]}{E[\Delta'_{CS}^2]}}$
0.05	0.975	1.15	0.993	3.007	0.031	0.100	0.003	0.124	3.067	0.899
0.1	0.925	1.2	0.970	3.030	0.061	0.078	0.013	0.112	2.168	0.811
0.15	0.868	1.257	0.935	3.065	0.077	0.070	0.029	0.114	1.632	0.784
0.2	0.810	1.315	0.886	3.114	0.086	0.066	0.050	0.107	1.315	0.786
0.25	0.750	1.375	0.827	3.173	0.095	0.064	0.077	0.099	1.112	0.802
0.3	0.690	1.435	0.759	3.241	0.105	0.062	0.110	0.091	0.973	0.827
0.35	0.630	1.495	0.683	3.317	0.116	0.061	0.154	0.083	0.868	0.856
0.4	0.569	1.556	0.600	3.400	0.131	0.060	0.212	0.076	0.785	0.890
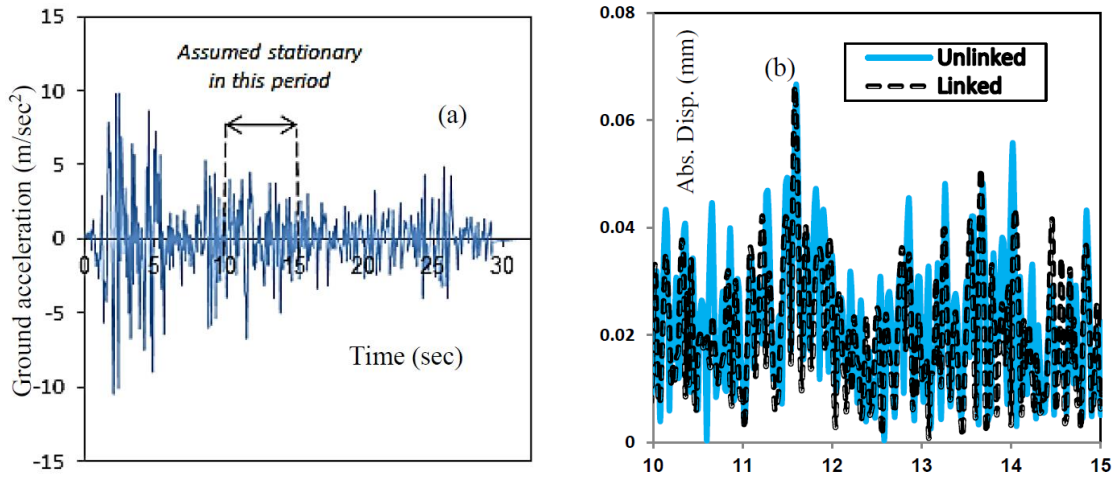
Fig. 2 (a) Scaled El Centro NS record (b) Absolute displacement-linked and unlinked asymmetric buildings

processes such as seismic events. Accordingly, the well-known NS component of the El Centro 1940 earthquake was first scaled to 1 g (Fig. 2(a)) and then applied to a couple of 2-DOF systems that are representatives of adjacent linked and unlinked asymmetric (with e'=0.2 and α=0.5) rigidly-connected identical buildings, respectively. The uncoupled lateral stiffness of the buildings was set to be ω_0=15 rad/s. The 5%-damped absolute displacement time histories are presented in Fig. 2(b) for a time interval that the input record can be assumed stationary, i.e., between 10 to 15 second. From the figure, it can be declared that not only the linked –to-unlinked response ratio roughly lies between 0.5 and 1, but it even seems to be generally scattered around 0.7 to 0.8 that is in acceptable agreement with the value of 0.786 obtained in Table 1 for e'=0.2 and α=0.5. Such a comparison can potentially confirm the appropriateness of white noise analysis for comparison of the results ratio between linked and unlinked cases.

Turning back to Table 1, it is observed that increasing the eccentricity ratio up to a critical value of 0.3 would increase the rotation in a decreasing rate compared to uncoupled case. This is in contrast to static analysis, where the rotation is expected to be reduced due to structural interconnection. More increase of the eccentricity, however, gradually reduces the rotation as a result of rigid linking. The displacement at the center of rigidity is less than the case of no connection between buildings for all possible eccentricities and since this displacement is proportional to the total base shear of a linear asymmetric building, it can be concluded that the torsional coupling can reduce the base shear of the identical rotationally-stiff connected structures, even to more than 20%, for moderate 10%-25% eccentricities.

Results for other two cases of α=0.2 and 0.35, together with α=0.5, are presented in Figs. 3 and 4 in the form of linked-to-unlinked response ratio, the former for rotation and the latter for displacement at the center of rigidity. A minimum eccentricity ratio of 0.05 is used, as buildings with lower eccentricities are not required to be calculated for torsion. As is clear from Fig. 3, case α=0.35 follows the same trend as α=0.5 for the comparison of rotation between linked and unlinked systems, but with a lower critical eccentricity, i.e., e'=0.16. For α=0.2, however, the rotation of linked structure is less than that for a separated building, regardless of eccentricities. It can also be concluded from Fig. 3 for α=0.35 that the base shear of the connected buildings is smaller than the corresponding value in unlinked building for eccentricity ratios less than 0.35 and the reverse would
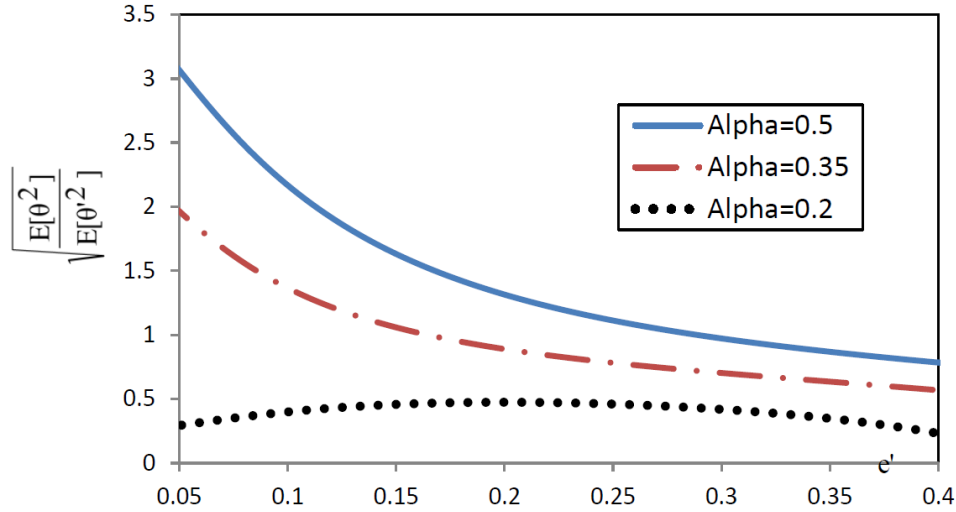
Fig. 3 linked-to-unlinked response (rotation) ratio with respect to the identical eccentricities of buildings

take place for higher eccentricities. On the other hand and for α=0.2, the displacement at the center of rigidity is always higher in linked structures than unlinked one resulting in higher total base shear. Prevention of base shear increase is desirable from the design point of view and this is achieved here for moderate to high values of α, especially when buildings are not highly eccentric. However, the reduction of base shear is more significant in the next parts of the study, where the difference of lateral stiffness (more accurately, frequencies) increases rotation-free base shear of the stiffer building with respect to the case without a connection.

In addition to the center of rigidity, we should also be concerned of the points with maximum lateral displacement on the plan, where the displacement due to the rotation is additive to central displacement. Considering the assumption of one-way eccentricity stated before, this would occur at an outer edge perpendicular to eccentricity. This edge is called the flexible edge and is distinguished in Fig. 1 for positive values of rotation and pure displacement. Displacement at flexible edge can be computed as follows, with the parameters defined before.

$$E[\Delta_{FE}{}^2] = E[U^2] + (b/2)^2 . E[\theta^2] + b..E[U.\theta] \quad (\textit{Use (') for separated building}) \qquad (12)$$

In Table 2, linked-to-unlinked response ratio for the displacement at the flexible edge has been presented for different eccentricities and torsional-to-lateral stiffness ratios, α. As is seen, the displacement at the flexible edge has never been increased as a result of the rigid in-between connection of buildings for α=0.2 and 0.35 and this is nearly true for α=0.5, except at minimum considered eccentricities.

In design of structures with asymmetric plans, an identical cross-section may be used for all columns in each story and this typical section assignment is usually based on the maximum base shear among the columns. This puts forward a significant advantage, in that the over-strength may exist in resisting elements distant from the flexible edge. Now, if the over-strength is defined as the ratio of displacement at the flexible edge to that at the center of rigidity, then an increase can be allowed for the total base shear of the asymmetric linear system. This is because the over-strength may counteract the increase of total base shear caused by the rigid connection. Though this
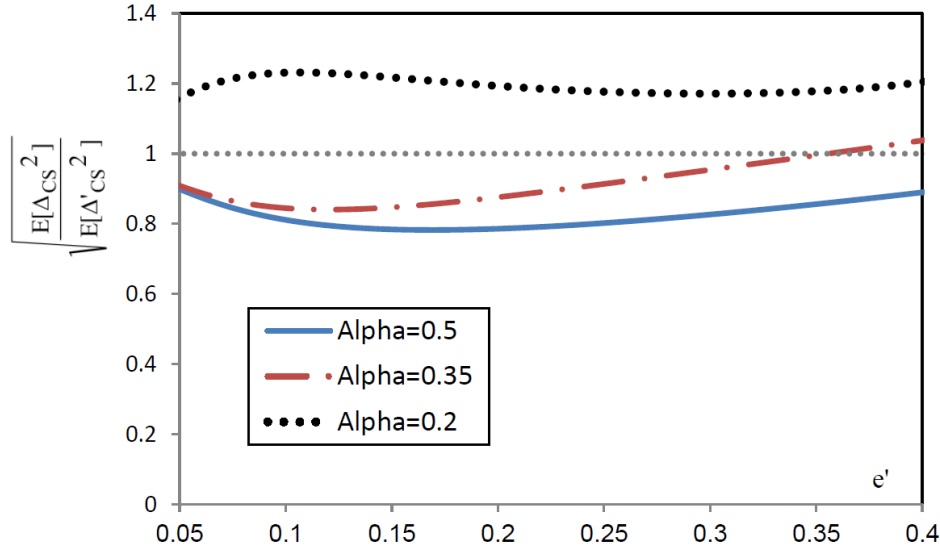
Fig. 4 linked-to-unlinked response (displacement at the center of rigidity) ratio with respect to identical eccentricities of buildings

Table 2 Linked-to-unlinked response (displacement at the flexible edge) ratio

$e'(=e'_1=e'_2)$	$\alpha=0.2$ Allowable shear increase due to over-strength of columns in typical section design	$\sqrt{\dfrac{E[\Delta_{FE}^{2}]}{E[\Delta'_{FE}^{2}]}}$	$\alpha=0.35$ $\sqrt{\dfrac{E[\Delta_{FE}^{2}]}{E[\Delta'_{FE}^{2}]}}$	$\alpha=0.5$ $\sqrt{\dfrac{E[\Delta_{FE}^{2}]}{E[\Delta'_{FE}^{2}]}}$
0.05	1.108	0.625	0.627	1.062
0.1	1.161	0.547	0.629	0.938
0.15	1.165	0.518	0.634	0.861
0.2	1.142	0.505	0.635	0.813
0.25	1.248	0.486	0.631	0.780
0.3	1.450	0.448	0.619	0.754
0.35	1.694	0.378	0.598	0.729
0.4	1.999	0.258	0.564	0.703

counteraction does not need to be mentioned for $\alpha=0.35$ and 0.5 due to the reduction of total base shear in these cases, the results for $\alpha=0.2$ is favorable as presented in the second column of Table 2. Comparing the column with Fig. 4 for the lower bound of α clearly demonstrates that the over-strength exceeds the increase of base shear for eccentricity ratios more than 0.25 and a positive effect of rigid linking is thus achieved in this low torsional stiffness condition that would be irrelevant for buildings without additional capacity of resisting elements, i.e., when each column is to be designed only against its load share.

4.2 Part B

In Tables 3 through 5, the linked-to-unlinked response ratio has been presented for different

eccentricities and lateral stiffness ratios of adjacent buildings, respectively for α=0.2, 0.35 and 0.5. Due to nearly unchanged effects on the trends of results, only a single torsional stiffness ratio is considered for each lateral stiffness ratio, with the same value of these ratios. This may be practically achieved if the buildings have a similar arrangement of columns. Furthermore, values less than unity were assigned to lateral stiffness ratio in order to focus on the more critical response corresponding to the stiffer building. It can be seen from Tables 3 to 5, regardless of $Kx2/Kx1$ and α, that the rotation ratio decreases by increasing the eccentricities of adjacent buildings. However, this ratio is more than unity for α=0.5 and also in most of the case for α=0.35 with the values between 0.3 to 0.75 times of those in α=0.5, denoting the negative effect of rigid connection on rotation in such cases. For α=0.2, the ratio is less than unity in most cases except for high eccentricities and for the highest lateral stiffness difference, i.e., $Kx2/Kx1$=0.01 .

The displacement response ratio, on the other hand, not only attains values more than unity for $Kx2/Kx1$=0.01 and 0.1, but increases for higher eccentricities of adjacent buildings. Note that for adjacent symmetric buildings, the linked-to-unlinked displacement ratios would be equal to 1.70 and 1.56, respectively for $Kx2/Kx1$ values of 0.01 and 0.1 and Comparing these values with Tables 3 to 5 for $Kx2/Kx1$=0.01 shows that the asymmetry of buildings can increase the base shear up to 12% and 34%, respectively for α values of 0.35 and 0.2. For α=0.5, albeit the displacement ratio is always less than the value for symmetric plans, but the maximum possible decrease due to plan eccentricities is about 14.5% and thus insufficient for preventing the base shear increase. The same trend is true for $Kx2/Kx1$=0.1, but with an interesting result that even a minimum eccentricity ratio of 0.05 increases the base shear by 18% for the flexible case of α=0.2. These observations confirm that rigid linking between buildings of high lateral stiffness differences would not make benefits and the torsional coupling even worsens the situation by putting the ratio into an increasing rate at higher eccentricities.

Furthermore, it is obvious from Tables 5-8 that shifting the lateral stiffness ratio towards unity reduces the increase of total base shear. Moreover and for α=0.5, up to 30% reduction is anticipated as a result of the asymmetry of linked plans by considering the rotation-free displacement increase of 42% for $Kx2/Kx1$=0.25. In spite of this, it would be desirable if the response ratio approaches values less than unity or very close to that in asymmetric structures and this is obtained here for $Kx2/Kx1$=0.5 and for α values 0.5 and 0.35, but not for α=0.2. For $Kx2/Kx1$=0.25, although the increase of base shear occurred as a result of the rigid connection, results for α=0.5 shows the potential to be marked accepted if a typical column section assignment mentioned in part A is taken into account. In Fig. 5, the corresponding over-strength of the columns located at the center of rigidity, together with the linked-to-unlinked response ratio for displacement at that center, are shown versus the eccentricity (assumed to be identical in both structures) of adjacent buildings. From the figure, it may be deduced that the over-strength can be more than the increase of base shear except for low values of eccentricities. Also in Fig. 5 are the linked- to-unlinked ratios of displacement at the flexible edge for $Kx2/Kx1$ values of 0.25 and 0.5. It can be seen for $Kx2/Kx1$=0.5 that the rigid connection decreases the flexible edge displacement at higher eccentricities. On the other hand and for $Kx2/Kx1$=0.25, this reduction would not take place, although the ratio is acceptably close to unity at higher values of eccentricity.

Proper results obtained in this part for the two closer-to-unity values of lateral stiffness ratio may encourage one to trace the condition by getting closer the lateral stiffness of buildings. This is the core of part C of the present study, where a building with stiffness no more than twice of that in its adjacent building is examined to seek cases with displacement responses less than the values of unconnected buildings. Contrary to part B, the stiffer building will be assumed symmetric in part C

Table 3 Linked-to-unlinked response ratio (rotation and displacement at the center of rigidity) for $\alpha=0.5$

e'_1	e'_2	Kx_2/Kx_1=0.01 ($K\theta2/K\theta1$=0.01)		Kx_2/Kx_1=0.1 ($K\theta2/K\theta1$=0.1)		Kx_2/Kx_1=0.25 ($K\theta2/K\theta1$=0.25)		$Kx2/Kx_1$=0.5 ($K\theta2/K\theta1$=0.5)	
		Rot.	Disp. Cent. Rigid.	Rot.	Disp. Cent. Rigid.	Rot.	Disp. Cent. Rigid.	Rot.	Disp. Cent. Rigid.
	0.05	4.376	1.606	5.435	1.435	5.917	1.200	4.359	1.079
0.05	0.1	4.411	1.604	5.731	1.415	6.325	1.163	5.005	1.035
	0.2	4.481	1.601	6.241	1.377	6.843	1.112	5.717	0.983
	0.05	3.553	1.507	3.738	1.318	3.536	1.113	2.736	0.998
0.1	0.1	3.563	1.505	3.800	1.305	3.604	1.100	2.882	0.978
	0.2	3.582	1.502	3.900	1.284	3.709	1.081	3.069	0.955
	0.05	2.900	1.449	2.813	1.277	2.529	1.098	2.014	0.970
0.15	0.15	2.908	1.447	2.854	1.265	2.578	1.088	2.114	0.956
	0.3	2.920	1.444	2.910	1.249	2.645	1.081	2.222	0.953
	0.1	2.455	1.434	2.284	1.275	2.005	1.110	1.633	0.967
0.2	0.2	2.459	1.433	2.308	1.268	2.038	1.107	1.685	0.965
	0.4	2.468	1.430	2.356	1.258	2.106	1.107	1.786	0.977
	0.05	2.149	1.449	1.929	1.346	1.657	1.142	1.340	0988
0.25	0.15	2.152	1.448	1.948	1.300	1.684	1.139	1.379	0.987
	0.25	2.155	1.447	1.968	1.295	1.713	1.139	1.419	0.990
	0.35	2.158	1.446	1.988	1.291	1.743	1.141	1.462	0.997
	0.1	1.940	1.481	1.702	1.340	1.440	1.178	1.165	1.014
0.3	0.2	1.943	1.480	1.721	1.337	1.467	1.178	1.201	1.017
	0.3	1.945	1.480	1.740	1.334	1.496	1.180	1.238	1.023
	0.05	1.787	1.525	1.518	1.387	1.256	1.222	1.003	1.048
0.35	0.2	1.792	1.525	1.314	1.235	1.295	1.221	1.050	1.051
	0.35	1.797	1.524	1.577	1.382	1.341	1.225	1.106	1.061

as mentioned before.

4.3 Part C

In this last part of the study, a symmetric stiffer building is assumed to be rigidly-linked to a more flexible asymmetric one. This part provides the opportunity to challenge whether the asymmetry of the adjacent building can overcome the inefficiency due to rigid connection of 2D building or not. Similar to part B, torsional stiffness ratio of each building was adopted to be equal to the lateral stiffness ratio. Keeping in mind the aim of comparing base shears, displacement is the key response of interest in this part. In Table 6, the linked-to-unlinked displacement ratios are presented for different values of asymmetric building's eccentricity ratio, lateral stiffness ratio and identical torsional-to-lateral stiffness ratio, α, of adjacent buildings. In comparison to the part B of the study, values less than unity are more frequently obtained here for moderate to high values of α and for more than 20% eccentricity of the asymmetric building. For considered lateral stiffness ratios, total base shear reduction up to more than 20% is obtained compared to values for symmetric

Table 4 Linked-to-unlinked response (rotation and displacement at the center of rigidity) ratio for α=0.35

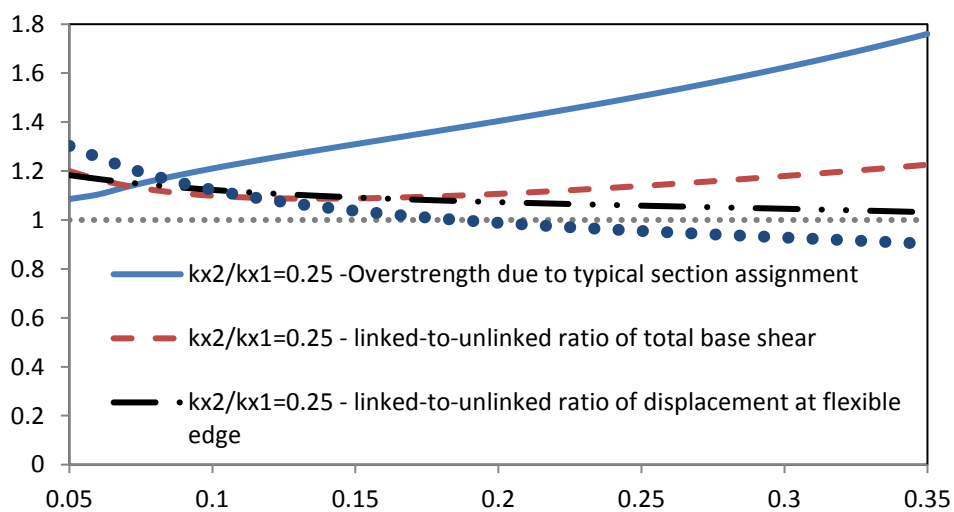| e'_1	e'_2	Kx_2/Kx_1=0.01 ($K\theta 2/K\theta 1$=0.01)		Kx_2/Kx_1=0.1 ($K\theta 2/K\theta 1$=0.1)		Kx_2/Kx_1=0.25 ($K\theta 2/K\theta 1$=0.25)		Kx_2/Kx_1=0.5 ($K\theta 2/K\theta 1$=0.5)	
		Rot.	Disp. Cent. Rigid.	Rot.	Disp. Cent. Rigid.	Rot.	Disp. Cent. Rigid.	Rot.	Disp. Cent. Rigid.
	0.05	1.602	1.672	1.730	1.553	1.981	1.382	2.195	1.160
0.05	0.1	1.617	1.671	1.871	1.505	2.288	1.356	2.608	1.105
	0.2	1.647	1.670	2.141	1.529	2.801	1.301	3.120	1.023
	0.05	1.558	1.682	1.553	1.546	1.576	1.354	1.520	1.126
0.1	0.1	1.565	1.681	1.607	1.536	1.674	1.327	1.632	1.084
	0.2	1.577	1.679	1.710	1.516	1.837	1.280	1.785	1.028
	0.05	1.515	1.704	1.429	1.556	1.349	1.355	1.214	1.131
0.15	0.15	1.522	1.702	1.484	1.537	1.433	1.314	1.302	1.078
	0.3	1.533	1.699	1.560	1.508	1.537	1.267	1.395	1.038
	0.1	1.478	1.736	1.349	1.575	1.221	1.365	1.061	1.140
0.2	0.2	1.484	1.735	1.384	1.558	1.268	1.336	1.108	1.108
	0.4	1.500	1.731	1.450	1.529	1.357	1.297	1.200	1.085
	0.05	1.445	1.787	1.252	1.622	1.079	1.421	0.907	1.202
0.25	0.15	1.450	1.776	1.278	1.608	1.116	1.396	0.945	1.171
	0.25	1.454	1.775	1.304	1.595	1.152	1.375	0.982	1.152
	0.35	1.458	1.773	1.331	1.583	1.190	1.360	1.023	1.143
	0.1	1.421	1.823	1.191	1.661	0.996	1.456	0.820	1.233
0.3	0.2	1.425	1.822	1.214	1.649	1.028	1.438	0.851	1.211
	0.3	1.429	1.820	1.238	1.640	1.062	1.423	0.890	1.200
	0.05	1.395	1.873	1.105	1.715	0.886	1.516	0.709	1.296
0.35	0.2	1.402	1.872	1.140	1.701	0.931	1.490	0.754	1.262
	0.35	1.408	1.870	1.177	1.690	0.981	1.474	0.808	1.250

Fig. 5 linked-to-unlinked response ratio for α=0.5 with respect to the eccentricity of asymmetric building

Table 5 Linked-to-unlinked response (rotation and displacement at the center of rigidity) ratio for $\alpha=0.2$

e'_1	e'_2	$Kx_2/Kx_1=0.01$ ($K\theta2/K\theta1=0.01$)		$Kx_2/Kx_1=0.1$ ($K\theta2/K\theta1=0.1$)		$Kx_2/Kx_1=0.25$ ($K\theta2/K\theta1=0.25$)		$Kx2/Kx_1=0.5$ ($K\theta2/K\theta1=0.5$)	
		Rot.	Disp. Cent. Rigid.	Rot.	Disp. Cent. Rigid.	Rot.	Disp. Cent. Rigid.	Rot.	Disp. Cent. Rigid.
	0.05	0.388	1.974	0.357	1.847	0.347	1.670	0.340	1.445
0.05	0.1	0.392	1.974	0.388	1.842	0.412	1.657	0.440	1.418
	0.2	0.399	1.973	0.450	1.833	0.535	1.626	0.610	1.354
	0.05	0.594	2.184	0.513	2.036	0.462	1.833	0.411	1.584
0.1	0.1	0.597	2.183	0.535	2.029	0.505	1.814	0.474	1.548
	0.2	0.603	2.182	0.580	2.013	0.585	1.773	0.580	1.477
	0.05	0.786	2.233	0.649	2.076	0.556	1.864	0.473	1.611
0.15	0.15	0.791	2.232	0.685	2.060	0.619	1.821	0.557	1.538
	0.3	0.799	2.229	0.738	2.031	0.706	1.760	0.658	1.449
	0.1	0.941	2.228	0.754	2.060	0.631	1.834	0.530	1.571
0.2	0.2	0.946	2.226	0.784	2.041	0.678	1.793	0.588	1.508
	0.4	0.956	2.223	0.847	2.007	0.772	1.725	0.693	1.426
	0.05	1.050	2.212	0.776	2.051	0.610	1.840	0.483	1.647
0.25	0.15	1.055	2.210	0.804	2.034	0.649	1.802	0.541	1.586
	0.25	1.061	2.208	0.833	2.017	0.690	1.767	0.578	1.486
	0.35	1.066	2.207	0.863	2.002	0.731	1.737	0.624	1.451
	0.1	1.123	2.198	0.774	2.031	0.584	1.814	0.457	1.567
0.3	0.2	1.130	2.197	0.801	2.016	0.619	1.871	0.494	1.516
	0.3	1.136	2.196	0.830	2.002	0.655	1.753	0.533	1.477
	0.05	1.144	2.202	0.678	2.043	0.475	1.840	0.355	1.608
0.35	0.2	1.157	2.200	0.719	2.021	0.518	1.792	0.398	1.533
	0.35	1.170	2.198	0.763	2.003	0.568	1.756	0.448	1.483

plans that presented in the second column of Table 6. It is also evident from this Table that reducing in total base shear is more pronounced for lateral stiffness ratios closer to unity. However, lower probability of collision should be considered in such cases that may affect the necessity of rigid linking for pounding mitigation purpose.

The reduction of total base shear would be guaranteed by just reducing the displacement at the center of rigidity and no more control is needed for a separated symmetric building. However, the torque transferred from the adjacent asymmetric building and the subsequent rotation leaves it mandatory to also check the displacement at the flexible edge. Accordingly, Results for the linked-to-unlinked ratio of displacement at the flexible edge are tabulated in Table 7. As is observed, the ratio is less than unity for a moderate value of $\alpha=0.35$, but more than 1.2 for the case of $\alpha=0.5$. For $\alpha=0.2$, results fall between the cases of $\alpha=0.35$ and 0.5 and the ratio decreases by getting closer the lateral stiffness of adjacent buildings. It is interesting to notice that a uniform pure displacement would happen for a single symmetric building and values less than unity in Table 7 thus indicate that integrating the buildings is even unable to increase the displacement at the points with maximum effect of in-plane rotation, a desirable result that is achieved in this part of the study. It can be concluded from Tables 6 and 7 that rigid connection to a moderately less stiff structure having

Table 6 Linked-to-unlinked response (displacement at the center of rigidity) ratio ($e'_1=0$)

α	-	0.2			0.35			0.5		
e'_2	0	0.1	0.2	0.3	0.1	0.2	0.3	0.1	0.2	0.3
$K_{x2}/K_{x1}=0.5$	1.241	1.223	1.177	1.121	1.175	1.066	0.991	1.159	1.056	1.001
$K_{x2}/K_{x1}=0.6$	1.182	1.159	1.103	1.041	1.096	0.980	0.917	1.103	1.005	0.956
$K_{x2}/K_{x1}=0.7$	1.130	1.102	1.038	0.973	1.030	0.912	0.861	1.050	0.958	0.914

Table 7 Linked-to-unlinked response (displacement at flexible edge) ratio ($e'_1=0$)

α	-	0.2			0.35			0.5		
e'_2	0	0.1	0.2	0.3	0.1	0.2	0.3	0.1	0.2	0.3
$K_{x2}/K_{x1}=0.5$	1.241	1.141	1.054	1.005	0.969	0.907	0.952	1.454	1.355	1.301
$K_{x2}/K_{x1}=0.6$	1.182	1.069	0.979	0.945	0.876	0.873	0.942	1.372	1.295	1.253
$K_{x2}/K_{x1}=0.7$	1.130	1.007	0.918	0.900	0.813	0.852	0.931	1.303	1.237	1.204

moderate to high plan eccentricity and low to moderate torsional stiffness would be more beneficial than leaving a symmetric building alone, since it reduces the base shear of columns and simultaneously keeps the buildings safe from local or global damages due to structural collision that otherwise needs to be analytically modeled by an impact spring at least 20 times stiffer than the symmetric building, as indicated by Anagnostopoulos (1988). Such a result deserves to be highlighted, recalling the fact that the reduction in the base shear of stiffer building would never occur for rigid connection of symmetric plans.

5. Conclusions

In this paper, the influence of rigid linking on the elastic lateral-torsional random responses of two adjacent one-story buildings has been investigated in three separate parts. Two identical asymmetric buildings were studied in part A, whereas part B dealt with buildings of different eccentricities as well as different lateral stiffness and torsional-to-lateral stiffness ratios. As the third part of the study, a symmetric building was connected to an adjacent moderately less stiff building having various eccentricities and different lateral and torsional stiffness values. The following concluding remarks can be outlined:
• The rotation of linked identical structures with moderate to high torsional stiffness is less than separated responses of buildings for high eccentricities. For low torsional stiffness, the rotation unexceptionally decreases due to the connection.
• The displacement at the center of rigidity, and thus the total base shear of linear structures, would be reduced by connecting buildings with identical dynamic properties and with moderate to high torsional-to-lateral stiffness ratios. Further, although rigid connection increases the base shear by more than 20% in the case of relatively low torsional stiffness, the concept of typical column section assignment can make this increase counteracted with the over-strength of seismic load resisting columns.
• Rigid linking should be considered unfavorable if the adjacent buildings have high lateral stiffness differences. Results reveal that torsional coupling is not only unable to prevent the base shear increase in stiffer building in such cases, but leads to an increasing trend in linked-to-

unlinked displacement ratio at high eccentricities.

• As the lateral stiffness ratio of the adjacent asymmetric buildings moves toward unity, results turn out to become more and more relaxed as compared to the case with considerable lateral stiffness differences. For high torsional rigidity, this occurs to an extent that the total base shear of an asymmetric building having typical column section assignment decreases when rigidly connected to an adjacent building four times, or less, more flexible. However, the increase of the displacement at the flexible edge should be controlled in such cases that might create a critical condition for columns located near that edge.

• The base shear reduction is achieved when a symmetric building is linked to a more than half stiff asymmetric one with low to moderate torsional-to-lateral stiffness ratio. In such case, the displacement at flexible edge did not exceed the uniform displacement of the separated building, with the exception for small eccentricities and high values of torsional-to-lateral stiffness ratio.

Finally, it should be noted that the promising results obtained here for adjacent buildings with closer translational frequencies, in spite of the unsatisfactory results for systems with highly different lateral frequencies, can hopefully pave the way for future works with the aim of removing the undesirable aspects of rigid connection and also saving adjacent asymmetric buildings from negative effects of seismic pounding.

Acknowledgement

References

Abd-Elsalam, S., Eraky, A., Abd-El-Motalleb, H. and Abdo, A. (2012), "Control of adjacent isolated-buildings pounding using viscous dampers", *J. Am. Sci.*, **8**(12), 1251-1259.

Abdeddaim, M., Ounis, A. and Shirmali, M. (2017), "Pounding hazard reduction using a coupling strategy for adjacent buildings", *Proceedings of the 16th World Conference on Earthquake Engineering*, Santiago, Chile, January.

Abdeddaim, M., Ounis, A., Djedoui, N. and Shirmali, M. (2016), "Reduction of pounding between buildings using fuzzy controller", *Asian J. Civil Eng.*, **17**(7), 985-1005.

Abdel Raheem, S.E., Ahmed, M.M.M., Ahmed, M.M. and Abdel Shafy, A.G.A. (2018), "Evaluation of the plan configuration irregularity effects on seismic response demands of L-shaped MRF buildings", *Bull. Earthq. Eng.*, **16**(9), 3845-3869. https://doi.org/10.1007/s10518-018-0319-7

Abdel Raheem, S.E., Fooly, M.Y.M., Abdel Shafy, A.G.A., Taha, A.M., Abbas, Y.A. and Abdel Latif, M.M.S. (2018), "Numerical simulation of potential seismic pounding among adjacent buildings in series", *Bull. Earthq. Eng.*, **17**(1), 439-471. https://doi.org/10.1007/s10518-018-0455-0.

Abdel Raheem, S.E., Fooly, M.Y.M., Omar, M. and Zaher, A.K.A. (2019), "Seismic pounding effects on the adjacent symmetric buildings with eccentric alignment", *Earthq. Struct.*, **16**(6), 715-726. https://doi.org/10.12989/eas.2019.16.6.715.

Ahmadi Taleshian, H., Mirzagoltabar Roshan, A. and Vaseghi Amiri, J. (2019), "Use of viscoelastic links for seismic pounding mitigation under random input", *Int. J. Struct.*. https://doi.org/10.1108/IJSI-06-2019-0055.

Ahmed, N.Z. and Abdel-Mooty, M.A.N. (2017), "Pounding mitigation in buildings using localized interconnections", *Proceeding of the World Congress on Advances in Structural Engineering and*

Mechanics, IIsun (Seoul), Korea, August-September.

Anagnostopolous, S.A., Kyrkos, M.T. and Stathopoulos, K.G. (2015), "Earthquake induced torsion in buildings: Critical view ans state of the art", *Earthq. Struct.*, **8**(2), 305-377. https://dx.doi.org /10.12989/ eas.2015.8.2.305.

Anagnostopoulos, S.A. (1988), "Pounding of buildings in series during earthquakes", *Earthq. Eng. Struct. Dyn.*, **16**, 443-456. https://doi.org/10.1002/eqe.4290160311.

Anagnostopoulos, S.A., Alexopoulou, C. and Stathopoulos, K.G. (2010), "An answer to an important controversy and the need for caution when using simple models to predict inelastic earthquake response of buildings with torsion", *Earthq. Eng. Struct. Dyn.*, **39**(5), 1813-1831. https://doi.org/10.1002/eqe.957.

Ban, S. (1973), "Earthquake interaction forces between two structures of different rigidities", *Earthq. Eng. Struct. Dyn.*, **2**, 133-141. https://doi.org/10.1002/eqe.4290020204.

Bharti, S.D., Dumne, S.M. and Shirmali, M.K. (2010), "Seismic response analysis of adjacent buildings connected with MR dampers", *Eng. Struct.*, **32**(8), 2122-2133. https://doi.org/10.1016/j.engstruct.2010.03.015.

Bycroft, G.N. (1960), "White noise representation of earthquakes", *J. Eng. Mech. Div.*, ASCE, **86**(2), 1-16.

Chakroborty, S. and Roy, R. (2016), "Seismic behavior of horizontally irregular structures: current wisdom and challenges ahead", *Appl. Mech. Rev.*, **68**, 1-17. https://doi.org/10.1115/1.4034725.

Chiba, M. and Magata, H. (2019), "Influence of torsional rigidity of flexible appendages on the dynamics of spacecrafts", *Coupl. Syst. Mech.*, **8**(1), 19-38. https://doi.org/10.12989/csm.2019.8.1.019.

Chopra, A.K. (1995), *Dynamics of Structures Theory and Application to Earthquake Engineering*, Prentice Hall, Englewood Cliffs, US.

Chouw, N. and Hao, H. (2005), "Study of SSI and non-uniform ground motion effect on pounding between bridge girders", *Soil Dyn. Earthq. Eng.*, **25**, 717-728. https://doi.org/10.1016/j.soildyn.2004.11.015.

Crandall, S.H. and Mark, W.D. (1963), *Random Vibration in Mechanical Systems*, Academic Press, New York.

Deng, Y., Guo, Q. and Xu, L. (2018), "Effects of pounding and fluid-structure interaction on seismic response of long-span deep-water bridge with high hollow piers", *Arab. J. Sci. Eng.*, **44**(5), 4453-4465. https://doi.org/10.1007/s13369-018-3459-9.

Hu, G., Tse, K.T., Song, J. and Liang, S. (2017), "Performance of wind-excited linked building systems considering the link-induced structural coupling", *Eng. Struct.*, **138**, 91-104. https://doi.org/ 10.1016/j.engstruct.2017.02.007.

Ibrahimbegovic, A. and Ademovic, N. (2019), *Nonlinear Dynamics of Structures under Extreme Transient Loads*, CRC Press, Taylor & Francis Group.

Ibrahimbegovic, A. and Mamouri, S. (2000), "On rigid components and joint constraints in nonlinear dynamics of of flexible multibody systems employing 3d geometrically exact beam model", *Comput. Meth. Appl. Mech. Eng.*, **188**(4), 805-831. https://doi.org/10.1016/S0045-7825(99)00363-1.

Ibrahimbegovic, A., Davenne, L., Markovic, D. and Dominguez, N. (2014), *Performance Based Earthquake-Resistant Design: Migration Towards Nonlinear Models and Probabilistic Framework*, Ed. Fischinger, M., Performance Based Seismic Engineering-Vision For Earthquake Resilient Society, Springer.

Imamovic, I., Ibrahimbegovic, A. and Mesic, E. (2018), "Coupled testing-modeling approach to ultimate state computation of steel structures with connections for statics and dynamics", *Coupl. Syst. Mech.*, **7**(5), 555-581. https://doi.org/10.12989/csm.2018.7.5.555.

Izharulhaque, Q. and Shinde, S. (2016), "Study of pounding mitigation techniques by use of energy dissipation devices", *Int. J. Civil Eng. Technol.*, **7**(4), 422-431.

Jankowski, R. and Mahmoud, S. (2015), *Earthquake-Induced Structural Pounding*, GeoPlanet, Earth Plan. Sci. Springer Int. Pub., Switzerland.

Jankowski, R. and Mahmoud, S. (2016), "Linking of adjacent three-story buildings for mitigation of structural pounding during earthquakes", *Bull. Earthq. Eng.*, **14** (11), 3075-3097. https://doi.org/10.1007/s10518-016-9946-z.

Jin, N. and Yang, Y. (2018), "Optimizing parameters for anticollision systems between adjacent buildings under earthquakes", *Shock Vib.*, **2018**, Article ID 3952495, 10.

Kandemir-Mazanoglu, E.C. and Mazanoglu, K. (2017), "An optimization study for viscous dampers between adjacent buildings", *Mech. Syst. Signal Pr.*, **89**, 88-96. https://doi.org/10.1016/j.ymssp.2016.06.001.

Kim, J., Ryu, J. and Chung, L. (2006), "Seismic performance of structures connected by viscoelastic dampers", *Eng. Struct.*, **28**, 183-195. https://doi.org/10.1016/j.engstruct.2005.05.014.

Leibovich, E., Rutenberg, A. and Yankelevski, D.Z. (1996), "On eccentric seismic pounding of symmetric buildings", *Earthq. Eng. Struct. Dyn.*, **25**, 219-233. https://doi.org/10.1002/(SICI)1096-9845 (199603) 25:3<219::AID-EQE537>3.0.CO;2-H.

Luco, J.E. and De Barros, F.C.P. (1998), "Optimal damping between two adjacent elastic structures", *Earthq. Eng. Struct. Dyn.*, **27**, 649-659. https://doi.org/10.1002/(SICI)1096-9845(199807)27:7<649::AID-EQE748>3.0.CO;2-5.

Lutes, L.D. and Sarkani, S. (2004), *Random Vibrations: Analysis of Structural and Mechanical Systems*, Elsevier, Burlington, MA.

Miari, M., Choong, K.K. and Jankowski, R. (2019), "Seismic pounding between adjacent buildings: Identification of parameters, soil interaction issues and mitigation measures", *Soil Dyn. Earthq. Eng.*, **121**, 135-150. https://doi.org/10.1016/j.soildyn.2019.02.024.

Mirzagoltabar Roshan, A., Ahmadi Taleshian, H. and Eliasi, A. (2017), "Seismic pounding mitigation by using viscous and viscoelastic dampers", *Proceedings of the International Conference of Scientist (ICS)*, Russia, July.

Nigam, N.C. (1983), *Introduction to Random Vibrations*, M.I.T. Press, Cambridge, MA.

Passoni, C., Belleri, A., Marini, A. and Riva, P. (2014), "Existing structures connected with dampers: State of the art and future developments", *Proceedings of the Second European Conference on Earthquake Engineering and Seismology*, Istanbul, Turkey, August.

Patel, C.C. and Jangid, R.S. (2010), "Seismic response of dynamically similar adjacent structures connected with viscous dampers", *The IES J: Civil Struct. Eng.*, **3**, 1-13. https://doi.org/10.1080/ 19373260903236833.

Perez, L., Avila, S. and Doz, G. (2017), "Experimental Study of the seismic response of coupled buildings models", *Proc. Eng.*, **199**, 1767-1772. https://doi.org/10.1016/j.proeng.2017.09.445.

Pratesi, F., Sorace, S. and Terenzi, G. (2014), "Analysis and mitigation of seismic pounding of a slender R/C bell tower" *J. Eng. Struct.*, **73**, 23-34. https://doi.org/10.1016/j.engstruct.2014.04.006.

Soltysik, B., Falborski, T. and Jankowski, R. (2017), "Preventing of earthquake-induced pounding between steel structures by using polymer elements- Experimental study", *Proc. Eng.*, **199**, 278-283.

Takewaki, I. (2013), *Critical Excitation Methods in Earthquake Engineering*, Second Edition, Elsevier, Oxford, U,.

Wang, L.X. and Chau, K.T. (2008), "Chaotic seismic torsional pounding between two single-story asymmetric towers", *The 14th World Conference on Earthquake Engineering*, Beijing, China.

Westermo, B.D. (1989), "The dynamics of interstructural connection to prevent pounding", *Earthq. Eng. Struct. Dyn.*, **18**, 687-699. https://doi.org/10.1002/eqe.4290180508.

Xu, Y.L., He, Q. and Ko, J.M. (1999), "Dynamic response of damper-connected adjacent buildings under earthquake excitation", *Eng. Struct.*, ASCE, **129**, 197-205. https://doi.org/10.1016/S0141-0296(97)00154-5.

Zhu, H. and Iemura, H. (2000), "A study of response control on the passive coupling element between two parallel structures", *J. Struct. Eng. Mech.*, **9**, 383-396. https://doi.org/10.12989/sem.2000.9.4.383.

Zhu, H.P. and Xu, Y.L. (2005), "Optimum parameters of Maxwell model-defined dampers used to link adjacent buildings", *J. Sound Vib.*, **279**, 253-274. https://doi.org/10.1016/j.jsv.2003.10.035.

Appendix: Notes in the derivation of Eq. (1)

In Eq. (1), the total moment of inertia about the center of mass of the left plan is set equal to $I_1+I_2+m_2.L^2$. The first two terms of this expression may be determined for any geometrical shape and are equal to $m.(b^2+d^2)/12$ for rectangular plans. The last term, however, needs to be explained more. Fig. 1A shows two masses rigidly linked together by a central distance of L between them. We may suppose that the collection is rotated around a fixed point and this point divides the connecting line into two parts, namely L_1 and L_2. In such a case, the mass moment of area about the center of mass m_1 would be as follows

$$Io = m_2 \left[(L_2 + L_1.\cos\theta)^2 + (L_1.\sin\theta)^2 \right] + m_1.L_1^2 \left[\sin^2\theta + (1-\cos\theta)^2 \right] \tag{A.1}$$
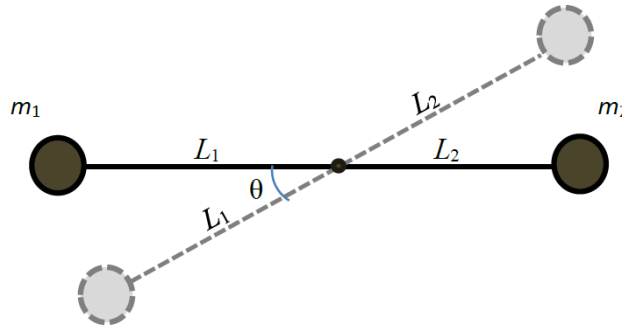

Fig. 1A Two masses connected by a rigid link

By extending this expression and recalling that $L_1+L_2=L$, we have

$$Io = m_2.L^2 + 4.L_1.(m_1.L_1 - m_2.L_2).\sin^2(\frac{\theta}{2}) \tag{A.2}$$

If the fixed point coincides with the mass centroid of the collection, then we have $m_1.L_1=m_2.L_2$ and the second term of (A.2) vanishes. This term is also of the second order with respect to θ and can thus be ignored if the small deflection assumption holds. This would be equivalent to ignoring the total inertia of the system in the y direction. This, together with assuming unidirectional ground acceleration, means that we have no pure pseudo-static load in *y*-direction. As a result, the fixed point of the rotation is just sensitive to the stiffness of the systems supporting the masses, rather than the inertia of the masses. This implies that the equation $K_{y1}.L_1=K_{y2}.L_2$ approximately holds and a torque would be produced, with the arm equal to the distance between the mass centroids. The couple would be equal to $M_0= K_{y1}.L_1.L$ and may be simplified by omitting L_1 from $K_{y1}.L_1=K_{y2}.L_2$ and $L_1+L_2=L$ as follows:

$$M_0 = K_{y1}.\ K_{y2}.L^2/(K_{y1}+ K_{y2}) \tag{A.3}$$

This is the last term in the array (2, 2) of the stiffness matrix in Eq. (1). This term is then summed with the rotational stiffness of the individual plans that can be calculated easily for a lateral load resisting system.